

# **Integrating Solar Chimney, Trombe Wall, and PCM for Enhanced Energy Efficiency: A Climate-Based Comparative Study**

**Nima Ghorbani<sup>1</sup>, Amirhossein Khayyaminejad<sup>1</sup>, Amir Fartaj<sup>1</sup>**

<sup>1</sup>Department of Mechanical, Automotive, and Materials Engineering/University of Windsor  
401 Sunset Ave, Windsor, Ontario, Canada  
Ghorbni@uwindsor.ca; Khayyam@uwindsor.ca

**Abstract** - This study examines the integration of Solar Chimney (SC) and Trombe Wall (TW) with Phase Change Material (PCM) to enhance energy efficiency and indoor comfort across diverse climates. Using DesignBuilder 7.0.2 and the EnergyPlus simulation engine, the performance of the SC+TW+PCM system was investigated in Rio (hot and humid), Yazd (hot and dry), Lhasa (mild and dry), and Detroit (cold and snowy) to evaluate its effectiveness under varying climatic conditions. The results show that the SC+TW+PCM system is most beneficial in warm and humid climates that have higher solar radiation and wind speed. In Rio, the SC+TW+PCM system raised peak indoor temperatures by 3.6°C over the reference case (without SC, TW, and PCM) and reduced heating loads close to zero for about 10 hours. Moreover, Yazd with its high solar gains, with indoor temperatures reaching around 25°C and heating loads dropping from 478.85 kW to 416.52 kW by utilizing the SC+TW+PCM system. This indicates that the case 3 configuration (SC and TW integrated with PCM) effectively utilized the solar radiation, and windy climate conditions of Yazd to reduce energy demands and improve thermal comfort. In Lhasa, a mild and dry climate, the system showed moderate improvements, decreasing heating loads by about 108.57 kW. However, in Detroit, the SC+TW+PCM configuration was less effective due to low solar gains and high heating demands, with minimal improvement in indoor temperature and a slight increase in heating load to 2095.9 kW from 2041.66 kW in Case 1. The findings highlight the case 3 system's efficiency in climates with higher solar gains and warmer temperatures, where passive heating and natural ventilation systems can be maximized. In warmer cities like Rio and Yazd, the system's ability to maintain higher indoor temperatures and reduce heating loads underscores its potential for renewable energy and sustainable building designs.

**Keywords:** Solar Chimney, Trombe Wall, Passive Heating, PCM, Natural Ventilation, Renewable Energy

## **1. Introduction**

Buildings consume a significant amount of energy, about 48% worldwide, and a significant portion of that energy is dedicated to maintaining indoor comfort [1]. Given that modern humans spend a considerable amount of time indoors, ensuring comfort within buildings has become increasingly crucial. According to the American Society of Heating Refrigerating and Air Conditioning Engineers (ASHRAE) [2], thermal comfort is described as a mental state reflecting a person's satisfaction with the surrounding thermal conditions. Although this definition is straightforward and supported by over 50 years of research, thermal discomfort remains one of the most frequently reported issues in building environments [3]. Indoor comfort can be attained through various passive techniques in a naturally ventilated building or by employing active mechanical systems in an air-conditioned building [4]. A practical strategy to reduce the negative impact of energy consumption is to replace or downsize active mechanical systems with passive alternatives, such as geothermal, tidal, wind, and solar energy. Among these renewable sources, solar energy is preferred due to its global accessibility and higher energy density compared to other renewable options.

Passive solar heating and ventilation systems, like solar roofs, Solar Chimney (SC), and Trombe Wall (TW), have shown improvements in energy efficiency. These systems can achieve annual energy savings between 30% and 70%, depending on factors such as wall dimensions, orientation, insulation quality, glazing materials, and local climate conditions [5]. Improving thermal comfort and reducing energy consumption in residential buildings can be effectively accomplished with natural ventilation. Studies indicate that residential buildings with SC experience a significant decrease in daily air-conditioning energy usage, approximately 10%–20% less than traditional rooms [6]. Additionally, when operated optimally, SC can reduce operating costs by as much as 30% [8]. The passive heating mechanism operates by utilizing buoyancy to drive warm air upward, establishing a natural flow from the inlet to the outlet, where cooler, denser air replaces the rising warm air, sustaining continuous circulation [7]. This process, involving radiation, convection, and conduction, enhances indoor comfort while decreasing dependence on non-renewable heating sources.

The SC is a widely used passive ventilation system that functions through a thermo-siphoning air channel. In this system, thermal buoyancy serves as the primary force driving airflow, enhancing natural ventilation within buildings by utilizing solar thermal energy [9]. Solar energy heats the air in the SC, lowering its density and causing it to rise and leave the chimney. This flow draws fresh air into the room, enabling effective ventilation [8]. SCs come in a variety of designs. In 2016, Ahmed Abdeen Saleem et al. [11] demonstrated that their proposed SC, featuring a 45° angle, 1.4 m length, 0.6 m width, and a 0.20 m air gap, achieved an airflow rate consistent with ASHRAE Standard 62 (0.019 to 0.033 m<sup>3</sup>/s). The system showed 88.2% effectiveness during the day, indicating its suitability for enhancing indoor air quality in hot, arid climates. In 2014, Rabani et al. [12] experimentally investigated the performance of an inclined SC with a water spray system in a hot and arid climate. Wang et al. [13] performed a numerical study to determine optimal design conditions considering external wind effects. They discovered that the ideal chimney width ranges from 0.4 to 0.5 m, compared to a narrower range of 0.2 to 0.3 m when external wind effects are not considered. Khayyaminejad and Fartaj [14] showed that adding a PCM layer to a building equipped with an SC improved energy savings by 5% at peak temperatures and by 3.5% over a 24-hour period compared to a building without PCM integration. Additionally, Park and Battaglia [15] developed a predictive equation for SC ventilation to establish a relationship between small-scale and full-scale SC models. Their findings indicated that the small-scale model could effectively predict the airflow and thermal conditions found in larger buildings.

In the 1970s, French engineer Felix Trombe introduced the well-known passive solar heating concept called the "Trombe wall" [16]. This design offers several advantages, including a simple structure, minimal reliance on mechanical power, and low cost [17,18]. As solar radiation is absorbed by the absorber plate, the air in the channel heats up through natural convection. This process creates a thermal siphon effect, enabling air circulation between the channel and the indoor space without mechanical power, thereby functioning as the room's heating and ventilation system. One technique to enhance the TW's performance is through structural optimization, which includes improvements to the glass cover and channel [19,20]. In 1987, Drake [21] enhanced heat capacity by incorporating PCM wallboards. Later, Peippo et al. [22] determined that the ideal melting point for PCM should be 1-3°C above the average room temperature. Kong et al. [23] investigated a TW system using single and dual layers of microencapsulated PCMs across summer and winter scenarios, examining four operational modes for heating and ventilation. They found that, with dual PCM layers, the average room temperature decreased by 0.93°C in summer and increased by 6.6°C in winter, while heat flux was reduced by up to 92% in summer and 75.7% in winter. Zhou & Razaqpur [24] assessed a TW system featuring a vertical rotating wall with PCMs and insulation, which alternated between heating and cooling modes to optimize energy storage and indoor comfort. Their findings indicated that this dynamic PCM TW system enhanced energy savings by 25.3% and improved thermal efficiency by 79.8%.

This research offers a novel investigation into the integration of TW-PCM with vertical SC to evaluate their combined impact on indoor temperature and energy efficiency across diverse climatic conditions. The study focuses on winter performance in four distinct climates: Lhasa (mild and dry), Yazd (hot and dry), Detroit (cold and snowy), and Rio de Janeiro (hot and humid). By examining the effects of these systems on heating demand, indoor temperature regulation, and natural ventilation, the research provides a detailed understanding of their interactions within building envelopes. A key contribution of this study is identifying the climates that benefit most from the TW-PCM and SC combination, offering practical insights into optimizing building designs for improved energy efficiency and comfort. This approach also supports the selection of appropriate technologies tailored to local climatic conditions, promoting greater adoption of renewable energy sources such as solar power. Furthermore, the findings establish a foundation for future research into integrating renewable energy systems with HVAC solutions, emphasizing their potential to enhance energy performance and indoor comfort in sustainable building design.

## 2. Model Description

Figure 1 depicts the physical domain configuration examined in this study, with additional geographical characteristics of the different cities detailed in Table 1. The domain studied covers a square area of 100 m<sup>2</sup> with a height of 4 m and includes east- and west-facing fenestrations totalling 6 m<sup>2</sup>. A set-point temperature of 23 °C was used

to calculate heating loads. On the northern and southern facades, an SC and a TW integrated with PCM are installed, respectively. The SC, positioned on the north wall, has a square-shaped glass front with a surface area of  $4 \text{ m}^2$  and a height height of  $5 \text{ m}$ . Within the SC, a central wall, measuring  $10.8 \text{ m}^2$  and standing  $4 \text{ m}$  tall, is constructed with three layers: aluminium absorber walls on either side and a layer of Expanded Polystyrene (EPS) insulation in between. The aluminium absorber walls have a high thermal conductivity of around  $237 \text{ W/m} \cdot \text{K}$ , enable effective heat transfer, while while the EPS layer, with a low thermal conductivity of approximately  $0.035 \text{ W/m} \cdot \text{K}$ , provides insulation to minimize heat loss. This configuration maximizes solar radiation absorption, with the absorber layer dividing the SC's interior space into two channels, effectively heating the air trapped within. The absorber wall's thermal inertia maintains natural convection, even without direct sunlight, thereby increasing the rate of natural ventilation in the dining room effectively.

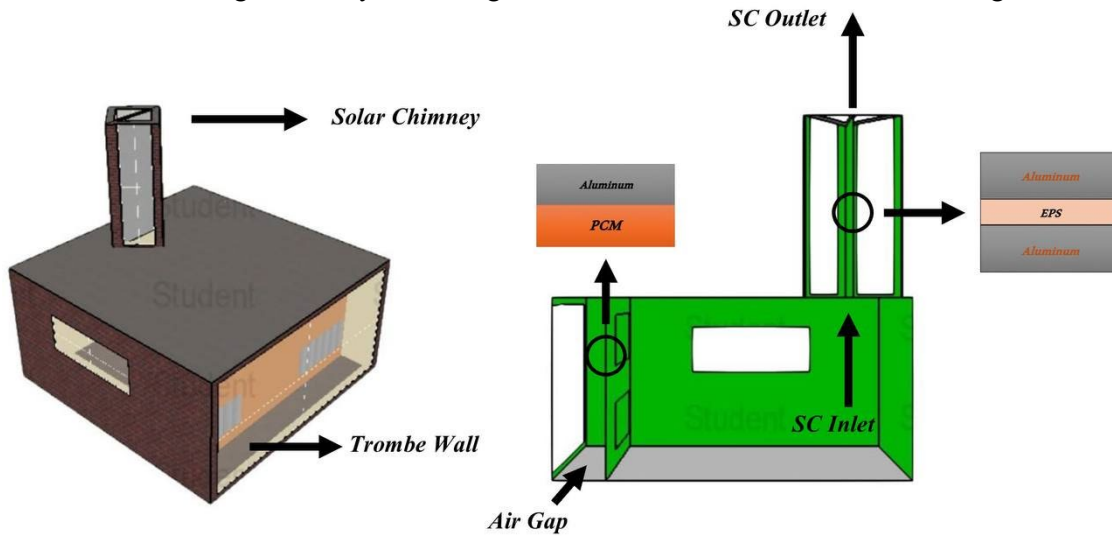


Fig. 1: Model 3D View.

Fig. 2: Unit Layout.

Table 1: Geographical characteristics of the investigated cities.

	Lhasa, China	Yazd, Iran	Detroit, USA	Rio, Brazil
Average wind speed (km/h)	5 to 10	10 to 15	11 to 16	10 to 15
Solar radiation (kWh/m <sup>2</sup> per day)	4.5 to 5.0	5.0 to 5.5	3.5 to 4.0	4.5 to 5.0
Average temperature (°C)	10	18	9	23
Geographic coordinates	29.6525° N, 91.1722° E	31.8974° N, 54.3670° E	42.3314° N, 83.0458° W	22.9068° S, 43.1729° W

The TW integrated with PCM is installed on the exterior wall, enhancing its functionality significantly within a large, open space by supporting improved natural ventilation across a wider area. The exterior layer of the TW consists of lightweight metallic cladding with a thickness of  $0.01 \text{ m}$ , followed by an air gap of  $0.5 \text{ m}$ . The interior surface is finished with  $0.05 \text{ m}$  of gypsum plaster. The roof's exterior layer is composed of  $0.05 \text{ m}$  of asphalt. On the floor, timber flooring is placed over the floor screed, with respective thicknesses of  $0.03 \text{ m}$  and  $0.07 \text{ m}$ . To drive buoyancy-driven airflow, outdoor air enters the air gap through a lower opening, where it heats up before circulating into the building through an upper opening. Figure 2 provides a schematic of the TW design, featuring an air gap with four grilles—two near the ceiling and two near the floor. The PCM used in this study is infinite RPCM  $18 \text{ }^\circ\text{C}$ . This material has a thermal conductivity of  $0.815 \text{ W/m} \cdot \text{K}$  and a density of  $929 \text{ kg/m}^3$ , utilizing a hysteresis phase change method. In its liquid phase, the PCM shows a thermal conductivity of  $0.54 \text{ W/m} \cdot \text{K}$ , a density of  $1540 \text{ kg/m}^3$ , and a specific heat capacity of  $3140 \text{ J/kg} \cdot \text{K}$ . In these analyses,

Case 1 represents the building without the integration of SC, TW, or PCM. Case 2 evaluates the building's performance when enhanced with the addition of TW and PCM, while Case 3 integrates a combination of SC and TW, along with PCM.

To configure the SC and TW within the DesignBuilder 7.0.2 simulation tool, it is essential to set the solar option to “Full Interior and Exterior” for accurate modeling of sunlight interactions on both the exterior and interior of the TW. Additionally, the zone type for the SC and TW should be specified as “Cavity,” which allows the software effectively simulate these elements as solar heat collectors. The simulation in this study employed the EnergyPlus engine, which underlies DesignBuilder and has been validated by multiple experimental studies [24]. For simulations without PCM, EnergyPlus’s standard Conduction Transfer Function (CTF) method was used [24]. EnergyPlus applies sophisticated algorithms for building physics, handling heat transfer (radiation, convection, and conduction), air and moisture movement, light distribution, and water flows, enabling simulation across a range of building types, system configurations, and environmental conditions with advanced features. For cases involving PCM, however, the Finite Difference method was utilized. This method, like the CTF approach, models heat transfer exclusively and does not account for moisture effects, making it highly suitable for accurate PCM simulations. A fully implicit, first-order scheme was employed for its stability, though it is known for being computationally slower [24]. This study focused on evaluating scenarios using only solar energy to boost natural ventilation, intentionally avoiding mechanical heating or ventilation systems. The aim was to improve comfort while reducing energy use and operational costs associated with continuous air conditioning. February 15th to 21st was selected for analysis as a winter week in Lhasa, Yazd, and Detroit based on regional weather data, however for Rio de Janeiro which is located in Brazil country July 15th to 21st was investigated.

### 3. Validation

The SC validation is presented in Figure 4, where the accuracy of the numerical simulations in this study is compared by comparison with the mathematical and numerical data from Saleem et al. [11]. Conducted under conditions similar to those examined by Mathur et al. [26] and Imran et al. [11], Saleem et al.’s study offers a basis for validation. Imran et al.’s [25] experimental setup included a room-measuring  $2\text{ m} \times 3\text{ m} \times 2\text{ m}$  with a solar chimney, consisting of a  $1\text{ mm}$  aluminium collector wall, a  $4\text{ mm}$  glass panel, and variable air gap thicknesses and tilt angles. A detailed comparison of Saleem et al.’s [9] results with the numerical data from this study, as shown in Figure 4, indicates strong alignment, confirming the reliability of the simulations. The maximum recorded error was 1.9% at hour 3.

Figure 3 presents the validation of the TW. The experimental study by Zhang et al. [25] was chosen to verify the accuracy of the numerical simulation. In their experiment, a TW was installed on the building's southern wall, with data recorded from April 23rd to April 25th. The study also incorporated PCM into the TW to examine its impact. As depicted in Figure 3, the numerical results closely align with the experimental findings, with a maximum error of 1.27% recorded on April 26th at 10:00 pm.

## 4. Results and Discussion

### 4.1 Dry-Bulb Temperature and Solar Gain

Fig.5 illustrates solar gains through exterior windows for the same four cities. Lhasa records the highest solar gains, with peak values reaching around 12 kW, closely followed by Yazd and Rio de Janeiro, with peak values of approximately 10 kW and 9 kW, respectively. Detroit experiences the lowest solar gains, peaking around 8 kW. Solar gains for all cities follow a cyclical pattern, with notable peaks during daylight hours and a sharp decline during nighttime, indicating the influence of solar exposure on heat gain. Higher solar gains are expected to enhance the passive heating effect, as increased solar energy absorption can promote air movement within the SC and TW structure.

Fig.6 displays the dry-bulb temperature trends for cities. Rio de Janeiro consistently experiences the highest dry-bulb temperatures, fluctuating around  $16^{\circ}\text{C}$  to  $20^{\circ}\text{C}$ . In contrast, Lhasa and Detroit exhibit more variable and lower temperatures. Lhasa’s temperatures generally fluctuate between  $-7^{\circ}\text{C}$  and  $8^{\circ}\text{C}$ , while Detroit's temperatures remain mostly between  $-5^{\circ}\text{C}$  and  $7^{\circ}\text{C}$ . Yazd shows a unique pattern, with temperatures peaking around  $15^{\circ}\text{C}$  and dipping below

2°C, indicating significant diurnal variation. The overall trend demonstrates Rio’s higher and more stable temperatures compared to the more fluctuating temperatures observed in the other cities. Given these dry-bulb temperature profiles, it is anticipated that cities with consistently higher dry-bulb temperatures, like Rio de Janeiro, would exhibit more pronounced impacts in Case 3. Higher outdoor dry-bulb temperatures increase the potential for heat transfer through building building walls, windows, and roofs, thus raising indoor temperatures.

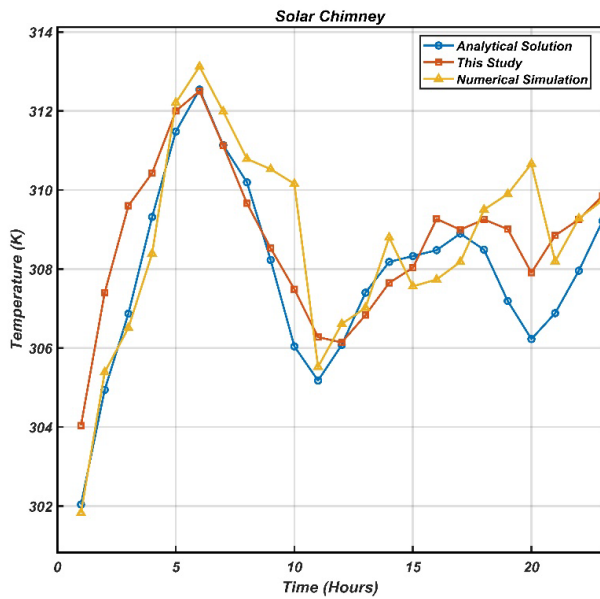


Fig. 3: SC temperature based on [11].

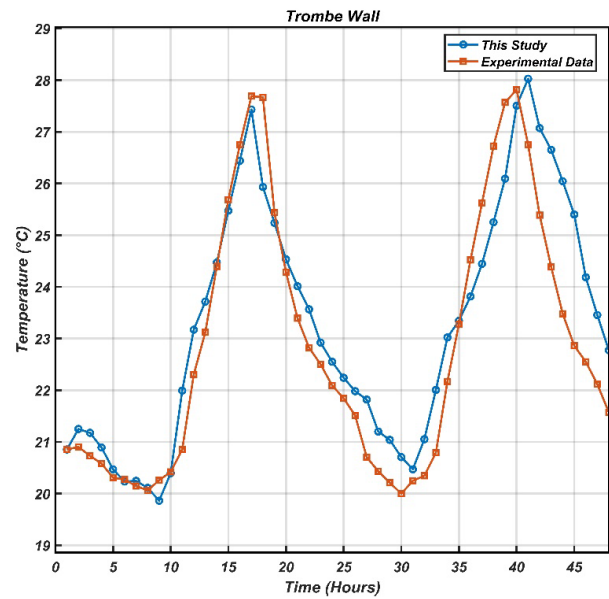


Fig. 4: TW temperature based on [25].

## 4.2 Indoor Temperature

Figures 7 to 10 demonstrate the variation in indoor temperature across different configurations. Among the cities analysed, the SC+TW+PCM configuration (Case 3) produces the greatest temperature difference in Rio de Janeiro City compared to Case 1. Figure 8 details fluctuations for Case 3, with indoor temperatures ranging from 21.6°C to 27.1°C, reaching a peak of 29.5°C and a minimum of 20.6°C. Additionally, this figure illustrates that, in Case 3, the peak indoor temperature is 3.6°C higher than in Case 1 and 3.0°C higher than in Case 2. These findings underscore the substantial impact of the Case 3 configuration in enhancing the indoor temperature of Rio de Janeiro.

In Figure 10, the temperature profiles for Case 1 and Case 2 reveal similar trends, with values generally fluctuating between 12°C and 20°C. Both cases follow a consistent cycle of peaks and valleys, reflecting a regular pattern of temperature increases and decreases. The highest temperature peak for both Case 1 and Case 2 reaches around 21°C, while the lowest points drop to approximately 11°C. Conversely, Case 3 demonstrates consistently higher temperatures, with peaks reaching up to 24°C. Although it begins with temperatures comparable to the other cases, Case 3 rises more sharply and shows noticeable deviations, especially during peak hours. The lowest temperature in Case 3 is around 12°C, maintaining a higher line even through the downward trends.

Figure 7 provides insights into indoor temperature fluctuations in Detroit City over 72 hours under three different cases. Temperatures across all three configurations remain relatively stable, mostly ranging between 4°C and 17°C. Notably, the temperature variations between cases are minimal, indicating that the different configurations have little effect on indoor temperatures. The peak temperature reached approximately 18°C in Case 3. However, Case 3 does not show a significant improvement over Cases 1 and 2, suggesting that this configuration may be less effective in cold and dry climates like Detroit.

Figure 8 highlights the indoor temperature trends in Yazd City, revealing temperature variations across the configurations compared to Detroit. Case 3 records the highest temperatures, peaking around 25°C. In contrast, Case 1

consistently shows the lowest temperatures, generally remaining between 16°C and 22°C. The distinct difference between Case 3 and the other cases suggests that the configuration in Case 3 is more effective in windy and warmer climates like Yazd, where higher ambient temperatures and solar gains help to raise indoor temperatures and enhance the passive heating effect.

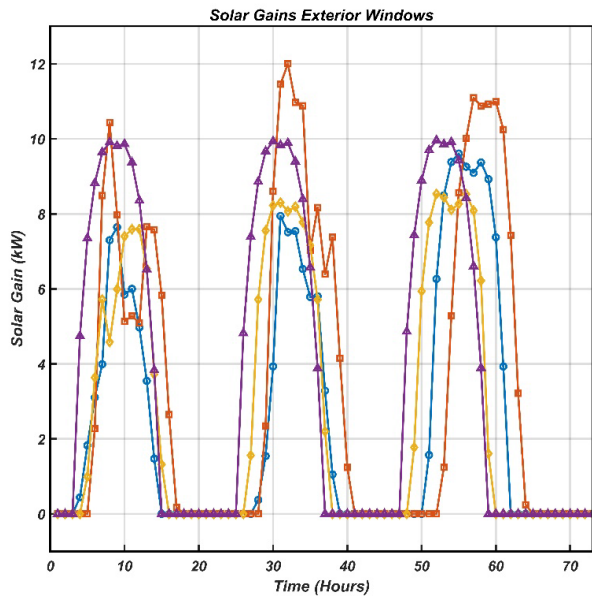


Fig. 5: Solar gains of windows in different cities

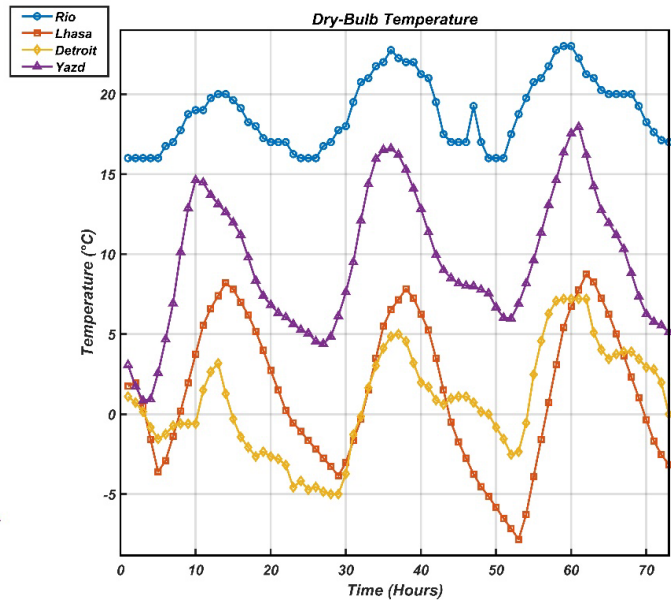


Fig. 6: Dry-Bulb temperature in different cities

### 4.3 Heating Load

The graphs illustrate the heating load variations across four cities comparing three different configurations. In Rio City (Fig. 9), the heating load in Case 3 is significantly reduced compared to Case 1. In Cases 1 and 3, the heating load reaches around 475 kW and 460 kW respectively. In case 3, the heating load drops close to zero during several intervals. For Lhasa City (Fig. 10), while Case 3 shows a reduction in heating load relative to Case 1, the decrease is not as pronounced as in Rio de Janeiro. Case 1 exhibits an average heating load of around 885.06 kW, while Case 3 reduces this to approximately 776.49 kW. However, Detroit City shows a slight rise in heating load with the Case 3 configuration compared to Case 1. In Case 1, Detroit's average heating load reaches about 2041.66 kW, while in Case 3, these peaks are reduced to around 2095.9 kW. In Fig. 8, Yazd City, the reduction in heating load for Case 3 is more noticeable than in Detroit but less than in Rio de Janeiro. Case 1's average heating load is approximately 478.85 kW, whereas Case 3 reduces these peaks to around 416.52 kW. Yazd's relatively warmer climate allows for more effective utilization of the SC+TW+PCM system. To conclude, all cities except Detroit (Fig. 7) experienced a decrease in heating load in Case 3 compared to Case 1, with the reduction being most significant in Rio de Janeiro, followed by Yazd, Detroit, and Lhasa. The effectiveness of the SC+TW+PCM configuration in reducing heating load is highly dependent on the local climate, with warmer cities seeing greater benefits.

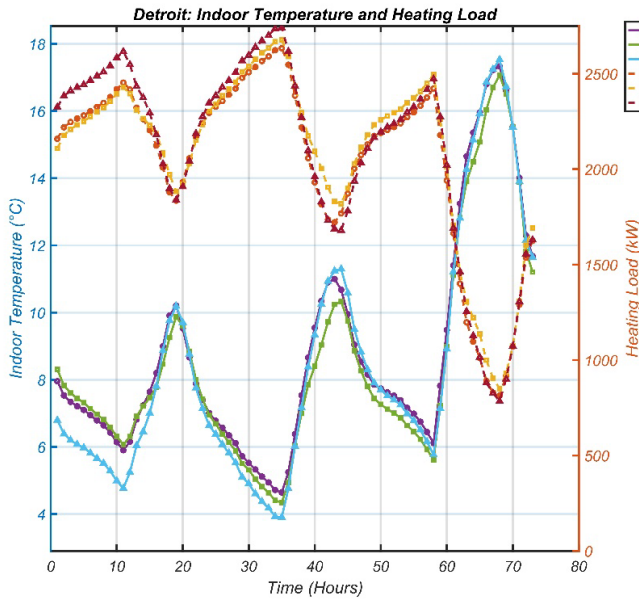


Fig. 7: Indoor air temperature and Heating load in Detroit.

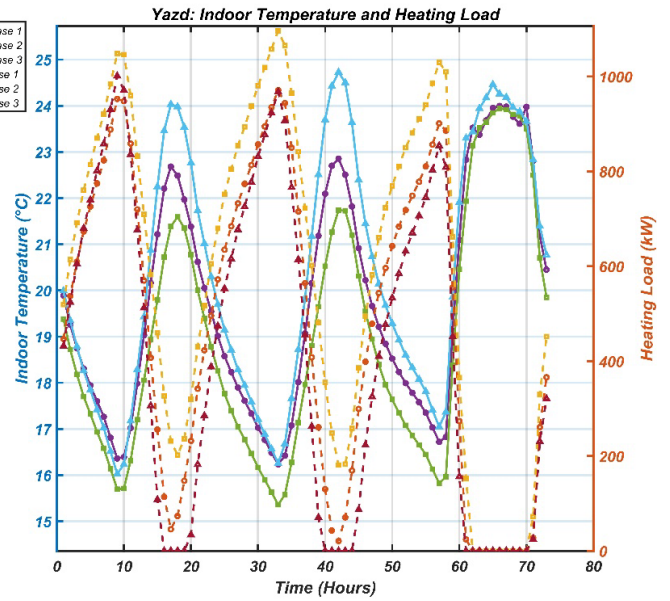


Fig. 8: Indoor air temperature and Heating load in Yazd.

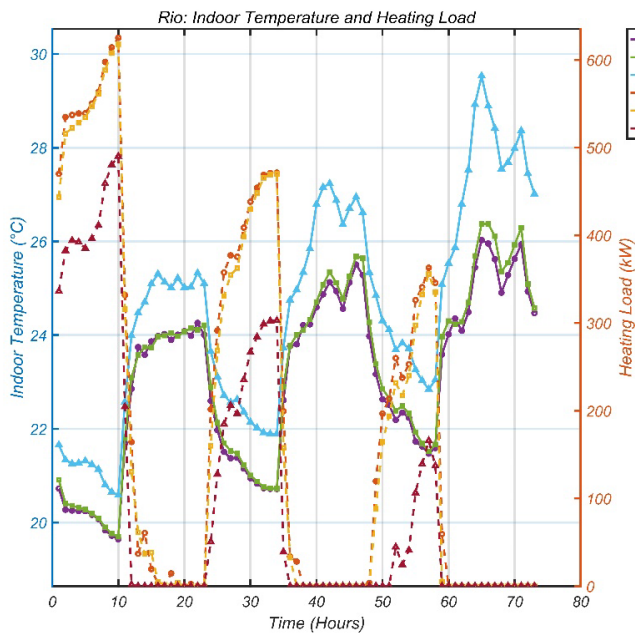


Fig. 9: Indoor air temperature and Heating load in Rio de Janeiro.

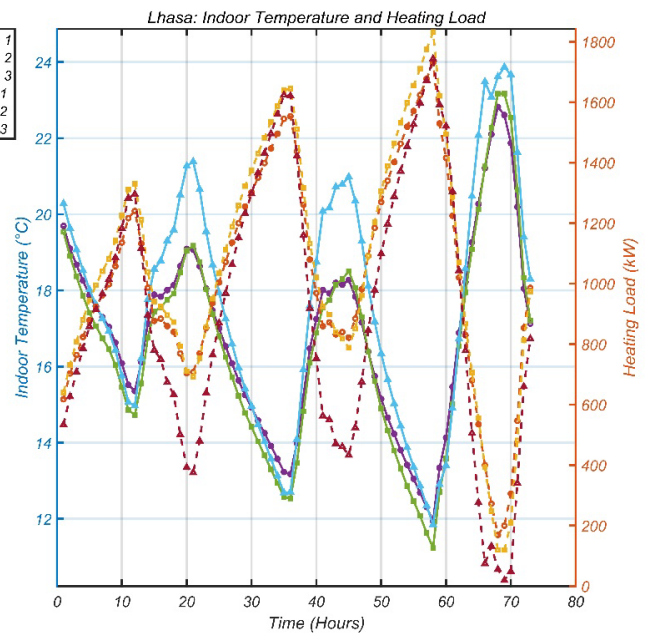


Fig. 10: Indoor air temperature and Heating load in Lhasa.

## 5. Conclusion

This study evaluated the integration of SC, TW, and PCM to enhance energy efficiency and indoor comfort across four distinct climates. Results show the system's effectiveness varies significantly with climatic conditions. In Rio de Janeiro, the SC+TW+PCM system raised indoor temperatures by 3.6°C compared to the baseline (Case 1), with peaks reaching 29.5°C,

and reduced heating loads to near zero for several hours. Yazd, benefiting from strong solar gains, maintained indoor temperatures around 25°C and reduced heating loads from 478.85 kW to 416.52 kW. Lhasa showed moderate with heating loads reduced by 108.57 kW. However, Detroit, with its cold and snowy climate, saw minimal impact, with heating loads increasing slightly in Case 3 to 2095.9 kW compared to 2041.66 kW in Case 1.

In warm and humid climates like Rio de Janeiro, High solar gains and mild outdoor temperatures enable the SC+TW+PCM system to perform optimally, reducing heating loads and achieving significant indoor temperature improvements. While in hot and dry climates in Yazd, strong solar radiation and large diurnal temperature swings provide conditions that enhance the system's efficiency. However, nighttime cooling and low ambient humidity require careful design adjustments. In contrast, in mild and dry climates like Lhasa, Moderate solar gains and cooler temperatures limit the system's overall impact. While there is some reduction in heating load, the benefits are less pronounced compared to warmer climates. On the other hand, in cold and snowy climates, Low solar radiation and high heating demands make the SC+TW+PCM system less effective. The additional energy required to maintain comfort outweighs the contributions of passive heating, particularly during extreme cold. It's worth mentioning that in cities like Rio and Yazd, wind patterns are more favorable for enhancing air circulation within the SC and TW, boosting the system's effectiveness. While, in Detroit, limited wind movement reduces the natural ventilation benefits of the SC, making the configuration less effective in improving indoor temperatures.

## References

- [1] BEE, ECBC. "Energy Conservation Building Code 2017." (2017).
- [2] Standard, A. S. H. R. A. E. "Thermal environmental conditions for human occupancy." ANSI/ASHRAE, 55 5 (1992).
- [3] Nicol, Fergus, Michael Humphreys, and Susan Roaf. *Adaptive thermal comfort: principles and practice*. Routledge, 2012.
- [4] Fundamentals, ASHRAE Handbook. "American society of heating." Refrigerating and Air-Conditioning Engineers (2005).
- [5] Sornek, Krzysztof, Karolina Papis-Frączek, Francesco Calise, Francesco Liberato Cappiello, and Maria Vicidomini. "A review of experimental and numerical analyses of solar thermal walls." *Energies* 16, no. 7 (2023): 3102.
- [6] Khayyaminejad, Amirhossein, and Amir Fartaj. "Efficient Cooling Approach with Integrated PCM Rooftops for Sustainable Load Reduction in Buildings with Natural Ventilation Systems." *Journal of Fluid Flow, Heat and Mass Transfer (JFFHMT)* 11, no. 1 (2024): 09.
- [7] Khayyaminejad, Amirhossein, Saman Jalilian, and Amir Fartaj. "Twisted tapes in solar chimney-earth air heat exchangers for equipment downsizing and passive cooling." *Journal of Building Engineering* 98 (2024): 111128.
- [8] Liu, Huifang, Peijia Li, Bendong Yu, Mingyi Zhang, Qianli Tan, Yu Wang, and Yi Zhang. "Contrastive analysis on the ventilation performance of a combined solar chimney." *Applied Sciences* 12, no. 1 (2021): 156.
- [9] Ali, Mahmud Hussain, Mahmood Khalid Mawlood, and Rawand Ehsan Jalal. "Investigation of the performance of a newly designed solar chimney for enhancing natural ventilation and mitigation of summer overheating." *Journal of Building Engineering* 95 (2024): 110310.
- [10] Zhai, X. Q., Z. P. Song, and R. Z. Wang. "A review for the applications of solar chimneys in buildings." *Renewable and Sustainable Energy Reviews* 15, no. 8 (2011): 3757-3767.
- [11] Saleem, Ahmed Abdeen, Mahmoud Bady, Shinichi Ookawara, and Ali K. Abdel-Rahman. "Achieving standard natural ventilation rate of dwellings in a hot-arid climate using solar chimney." *Energy and Buildings* 133 (2016): 360-370.
- [12] Rabani, Ramin, Ahmadreza K. Faghih, Mehrdad Rabani, and Mehran Rabani. "Numerical simulation of an innovated building cooling system with combination of solar chimney and water spraying system." *Heat and Mass Transfer* 50 (2014): 1609-1625. [13] Wang, Qingyuan, Guomin Zhang, Wenyuan Li, and Long Shi. "External wind on the optimum designing parameters of a wall solar chimney in building." *Sustainable Energy Technologies and Assessments* 42 (2020): 100842.
- [14] Khayyaminejad, Amirhossein, and Amir Fartaj. "Unveiling the synergy of passive cooling, efficient ventilation, and indoor air quality through optimal PCM location in building envelopes." *Journal of Energy Storage* 89 (2024): 111633.

- [15] Park, David, and Francine Battaglia. "Development of a predictive equation for ventilation in a wall-solar chimney system." *Journal of Solar Energy Engineering* 139, no. 3 (2017): 031001.
- [16] Sergei, Kostikov, Chao Shen, and Yiqiang Jiang. "A review of the current work potential of a trombe wall." *Renewable and Sustainable Energy Reviews* 130 (2020): 109947.
- [17] Wu, Shuang-Ying, Rong-Rong Yan, and Lan Xiao. "Numerically predicting the effect of fin on solar Trombe wall performance." *Sustainable Energy Technologies and Assessments* 52 (2022): 102012.
- [18] Yu, Bendong, Wei He, Niansi Li, Liping Wang, Jingyong Cai, Hongbing Chen, Jie Ji, and Gang Xu. "Experimental and numerical performance analysis of a TC-Trombe wall." *Applied energy* 206 (2017): 70-82.
- [19] Hernández-López, I., J. Xamán, Y. Chávez, I. Hernández-Pérez, and R. Alvarado-Juárez. "Thermal energy storage and losses in a room-Trombe wall system located in Mexico." *Energy* 109 (2016): 512-524.
- [20] Lal, Shiv. "Experimental, CFD simulation and parametric studies on modified solar chimney for building ventilation." *Applied solar energy* 50, no. 1 (2014): 37-43.
- [21] Drake, J. B. *A study of the optimal transition temperature of PCM wallboard for solar energy storage*. The Laboratory, 1987.
- [22] Peippo, K., Pertti Kauranen, and P. D. Lund. "A multicomponent PCM wall optimized for passive solar heating." *Energy and buildings* 17, no. 4 (1991): 259-270.
- [23] Kong, Xiangfei, Jinbo Li, Man Fan, Wei Li, and Han Li. "Study on the thermal performance of a new double layer PCM trombe wall with multiple phase change points." *Solar Energy Materials and Solar Cells* 240 (2022): 111685.
- [24] Zhou, Shiqiang, and A. Ghani Razaqpur. "CFD modeling and experimental validation of the thermal performance of a novel dynamic PCM Trombe wall: Comparison with the companion static wall with and without PCM." *Applied Energy* 353 (2024): 121985.
- [25] Zhang, Yuan, Ziyang Zhu, Zian Peng, Jing Luo, Xiaoqin Sun, Jie Li, and Fen Peng. "The Trombe wall equipped with PCMs for the enhancement of the indoor thermal quality." *Energy and Buildings* 297 (2023): 113407.
- [26] Mathur, Jyotirmay, and Sanjay Mathur. "Summer-performance of inclined roof solar chimney for natural ventilation." *Energy and Buildings* 38, no. 10 (2006): 1156-1163.
- [27] Imran, Ahmed Abdunabi, Jalal M. Jalil, and Sabah T. Ahmed. "Induced flow for ventilation and cooling by a solar chimney." *Renewable energy* 78 (2015): 236-244.